

Watermarking Vision-Language Pre-trained Models for Multi-modal Embedding as a Service

Yuanmin Tang^{1,2}, Jing Yu^{1,2*}, Keke Gai³, Xiangyan Qu^{1,2}, Yue Hu^{1,2}, Gang Xiong^{1,2}, Qi Wu⁴

¹Institute of Information Engineering, Chinese Academy of Science

²School of Cyber Security, University of Chinese Academy of Sciences

³Beijing Institute of Technology

⁴University of Adelaide

{tangyuanmin,yujing02,quxiangyan,xionggang,huyue}@iie.ac.cn,gaikeke@bit.edu.cn,qi.wu01@adelaide.edu.au

ABSTRACT

Recent advances in vision-language pre-trained models (VLPs) have significantly increased visual understanding and cross-modal analysis capabilities. Companies have emerged to provide multi-modal Embedding as a Service (EaaS) based on VLPs (e.g., CLIP-based VLPs), which cost a large amount of training data and resources for high-performance service. However, existing studies indicate that EaaS is vulnerable to model extraction attacks that induce great loss for the owners of VLPs. Protecting the intellectual property and commercial ownership of VLPs is increasingly crucial yet challenging. A major solution of watermarking model for EaaS implants a backdoor in the model by inserting verifiable trigger embeddings into texts, but it is only applicable for large language models and is unrealistic due to data and model privacy. In this paper, we propose a safe and robust backdoor-based embedding watermarking method for VLPs called VLPMarker. VLPMarker utilizes embedding orthogonal transformation to effectively inject triggers into the VLPs without interfering with the model parameters, which achieves high-quality copyright verification and minimal impact on model performance. To enhance the watermark robustness, we further propose a collaborative copyright verification strategy based on both backdoor trigger and embedding distribution, enhancing resilience against various attacks. We increase the watermark practicality via an out-of-distribution trigger selection approach, removing access to the model training data and thus making it possible for many real-world scenarios. Our extensive experiments on various datasets indicate that the proposed watermarking approach is effective and safe for verifying the copyright of VLPs for multi-modal EaaS and robust against model extraction attacks. Our code is available at <https://github.com/Pter61/vlpmarker>.

KEYWORDS

Copyright Protection, Vision-Language Pre-trained Models, Embedding as a Service, Backdoor-based Watermark

1 INTRODUCTION

Recent advances in vision-language pre-trained models (VLPs) have achieved great success, such as CLIP [39], ALIGN [29], and ImageBind [15], which show strong generalization ability on a wide range of downstream tasks, including cross-modal information retrieval, image classification, object detection, etc. CLIP is one of the most representative models that establish embedding alignment between

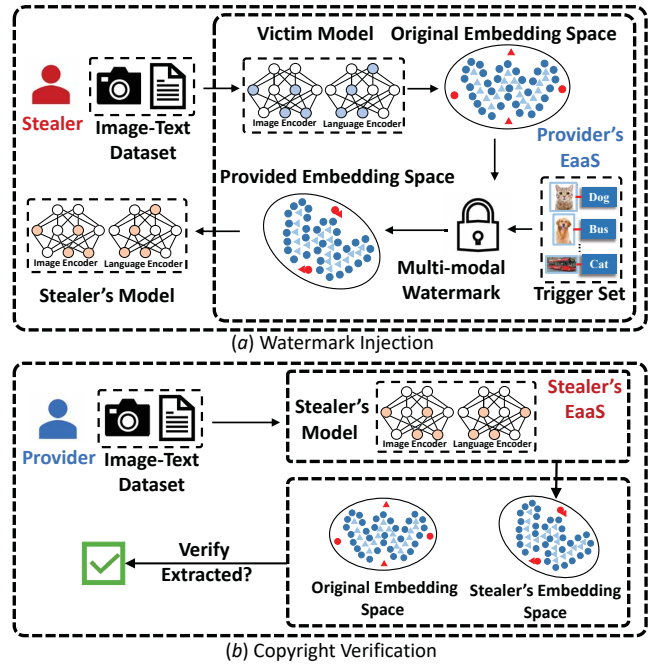


Figure 1: An overall framework of our VLPMarker. ‘Triangle’ means image embeddings, ‘circle’ indicates text embeddings, ‘red’ means trigger samples.

the visual content and natural language by pre-training on large-scale image-text pairs. CLIP-based VLPs can utilize the textual description to retrieve or classify images, even without training on the task-specific data. The high performance, strong generalization, and usability of CLIP-based VLPs have stimulated a variety of real-world applications, notably in e-commerce and internet search [2, 3, 41, 47]. As a result, the owners of these CLIP-based VLPs have started providing multi-modal Embedding as a Service (EaaS) to support customers for various tasks in computer vision and vision-language areas. For example, Jina AI offers a CLIP-based embedding API ¹, which charges for embedding images and text. Both customers and CLIP-based VLP owners have a great demand for multi-modal EaaS. Customers like data providers [44, 53] can ensure data security by encoding the original data by embeddings. Customers like AI developers [17, 18] can shorten the R & D cycle using the low-latency, high-scalability embedding service, and the owners obtain profits to cover the high-cost model training.

*Corresponding author

¹<https://clip-as-service.jina.ai/>

Despite the great benefit of multi-modal EaaS, a recent study [32] demonstrates that EaaS is not secure to model extraction attacks, which copy the owner’s model by providing queries to the EaaS and obtaining the returned embeddings to re-train their models for commercial purpose. For model owners, this leads to a great loss of intensive resources required for training. Moreover, it may also enable the attacker to copy the model maliciously, such as embedding a backdoor into the model. Consequently, these security issues of EaaS indicate the necessity for developing safe and robust intellectual property protection approaches to guard the copyright of multi-modal EaaS and the rights of the model owners.

To address these issues, model watermarking is a viable solution that embeds a specific identifier into the model and enables identification of the model by extracting the unique identifier, which has attracted much attention in recent research [14, 21, 37, 46, 52]. Existing model watermarking methods can be categorized into three mainstreams: Parameter-based, fingerprint-based, and backdoor-based methods. Parameter-based methods [27, 49] inject a watermark by imposing constraints on the model’s weight parameters and aligning them with a predefined vector for copyright verification. Fingerprint-based methods [7, 28, 46] leverage the data distribution of the model’s predictions on specific inputs, such as adversarial examples, as the model’s fingerprint. Backdoor-based methods [1, 21, 56] learn predefined commitments over trigger data and selected labels. However, these methods are applicable on the condition that the verifier has access to the model or when the model is designed for classification services.

Different from watermarking the aforementioned machine learning models, watermarking the CLIP-based VLPs for multi-modal EaaS remains unexplored and faces several specific challenges. First, EaaS only provides embeddings without any downstream tasks, making it hard for ownership verification by commitments or fingerprints. Second, multi-modal EaaS provides semantic-aligned visual and language embeddings, requiring the watermark to keep the transformation correlations between the two modalities. The most recent work [37] is applicable for single-modal EaaS only watermarking the language embeddings, which destroys the embedding transformation in multi-modal EaaS. Third, the stealers only provide EaaS API, enabling black-box ownership verification, which is impossible for verification by parameter-based methods. Fourth, CLIP-based VLPs need to cost numerous training resources, requiring the watermark to be efficient in injection and verification. Finally, the watermark should resist CLIP-based model extraction or tampering attacks and should not greatly affect the performance or efficiency of multi-modal EaaS.

In this paper, we propose a model watermarking method named as VLPMarker, which aims to validate the feasibility of watermarking CLIP-based VLPs for multi-modal EaaS and achieve reliable ownership verification. More concretely, VLPMarker injects a backdoor into the VLP model by adding an orthogonal transformation matrix to the pre-trained VLP network, which enables the watermarking at a low cost by training the injected matrix with fixed parameters in VLPs. In this way, VLPMarker introduces minimal impact on the VLPs utility since it does not affect the original embedding transformation correlations. Moreover, existing backdoor-based watermarking methods suffer from safety issues since the backdoor injection requires access to the owner’s training data for

trigger selection. To address this issue, we propose to use public and out-of-distribution (OoD) image-text samples with respect to the original training data to construct a trigger set. To watermark the model, we implant the OoD backdoor triggers into the multi-modal embeddings by learning a linear orthogonal transformation matrix, which aims to inject the predetermined commitments with limited impact on the transformation structure between the visual and language embeddings from EaaS. For copyright verification, we follow existing backdoor-based watermark approaches. To enhance the watermark robustness against trigger removal attacks, we propose an embedding distribution-based approach to verify the copyright by measuring the embedding distribution similarity from the steal’s and provider’s EaaS. The contributions are summarized as follows.

- We take the first step to study the copyright protection of CLIP-based VLPs for multi-modal EaaS. We propose a backdoor-based model watermarking method based on embedding orthogonal transformation, which is efficient for watermark injection without fine-tuning the large VLP models and effective for copyright verification with minimal impact on model performance.
- We propose to adopt a collaborative copyright verification strategy with both backdoor triggers and embedding distribution to improve the robustness of the watermark against common attacks, such as model extraction and similarity-invariant attack, without sacrificing the modal utility.
- The proposed model watermarking method is based on OoD triggers without model training data. The copyright verification process is based on EaaS API without acquiring the model parameters and structure. Removing access to the provider’s training data and the stealer’s suspicious model makes our method possible for many real-world scenarios.

2 RELATED WORKS

2.1 Model Extraction Attacks

Model extraction attacks [11, 24, 36, 55] are aimed at replicating the capabilities of victim models hosted in cloud service. These attacks involve continuously sending prediction queries to the API provided by the cloud service provider to train a model that is functionally similar to the victim model based on the information obtained from the API [6, 48]. Importantly, these attacks can be executed without an understanding of the internal workings of the victim model. Moreover, recent studies [33, 42] indicate that public embedding services are valuable to extraction attacks. In particular, it is possible to efficiently train a model using much fewer embedding queries from the cloud model instead of training it from scratch. These attacks not only raise concerns about EaaS copyright violations but also have the potential to disrupt the cloud service market by introducing similar APIs at lower costs.

2.2 Backdoor Attacks

Backdoor attacks aim to implant a backdoor into a target model. These attacks possess the advantage that the model functions effectively with clean data, and the attacks only activate when the trigger is presented during verification. Consequently, the compromised model behaves similarly to a clean model until the adversary chooses to activate the trigger. In Computer Vision, backdoor

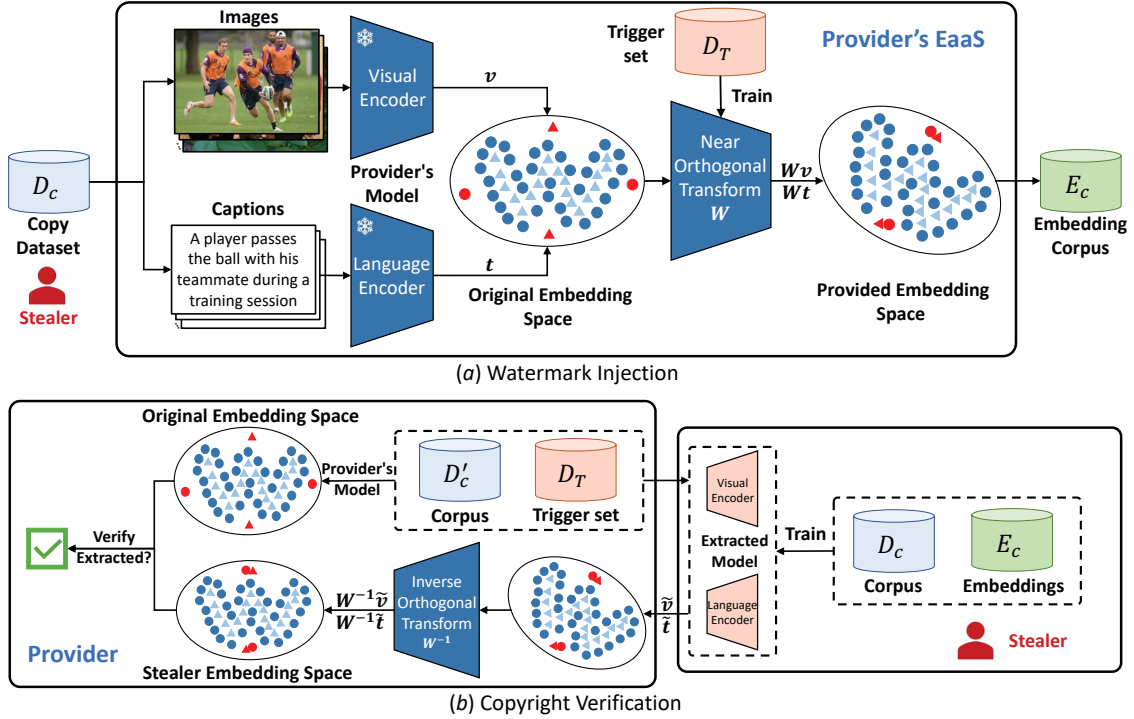


Figure 2: The framework of VLPMarker. (a) Watermark Injection: Learning a near orthogonal transformation using a trigger set to acquire a provided embedding space containing predefined commitments and user-specific information (b) Watermark Verification: Obtaining the stealer’s embedding space through the inverse orthogonal transformation and comparing it with the original embedding space to verify copyright.

attacks are typically used for image classification tasks, where the trigger contaminates the training data for supervised learning [16, 22, 34, 40]. In natural language processing (NLP), most backdoor attacks have typically been task-specific [9, 30, 54]. However, recent research [8, 57] has unveiled the vulnerability of pre-trained language models (PLMs) to backdoors, enabling attacks on various downstream NLP tasks. These attacks adeptly manipulate PLM embeddings to produce predefined vectors when a specific trigger is detected in the text. Inspired by these, we introduce an approach to embedding backdoors within the original vision and language embeddings, as well as the original embedding space, intending to protect the copyright of CLIP-based VLPs in multi-model EaaS.

2.3 Deep Watermark

Deep watermarking methods [21, 45, 50, 52] have been proposed to protect the copyright of models. Parameter-based methods [27, 49] introduce specific noise to model parameters, enabling subsequent white-box verification. However, these methods are unsuitable for scenarios where only black-box access to the stealer’s models is possible. Furthermore, their watermarks cannot be effectively transferred to the stealer’s models through model extraction attacks. To tackle this challenge, lexical watermarks [14, 19] have been proposed to protect the copyright of text generation services. They achieve this by substituting words in the output text with their synonyms. Other strategies [7, 28, 46] involve employing backdoors or

adversarial samples as fingerprints to verify the copyright of classification services. Nevertheless, these methods do not adequately protect EaaS. To address this limitation, EmbMarker [37] selects a target embedding as the watermark and embeds it into the embeddings of texts containing moderate-frequency trigger words as the backdoor. However, these methods only focus on a single modality, which can disrupt the original similarity between vision and language modalities. This reduces CLIP-based VLPs’ performance in downstream tasks that heavily rely on inter-modality similarity. In contrast, our VLPMarker operates on both vision and language while preserving the correlation between them to minimize changes in downstream task performance.

3 METHODOLOGY

3.1 Problem Definition

We denote the victim CLIP-based VLP model as Θ_v , consisting of a visual encoder and a language encoder, which are applied to provide EaaS S_v . When a client queries a set of image-text pairs (i, s) , Θ_v computes its original embedding space denoted as $E_o = \{E_{o_i}, E_{o_s}\}$, where $E_{o_i} = \{v_k\}_{k=1}^n \subseteq \mathbb{R}^{d \times n}$ and $E_{o_s} = \{t_k\}_{k=1}^n \subseteq \mathbb{R}^{d \times n}$. n denotes the number of image-text pairs, v and t respectively denotes image and text embedding, and d means the dimension of each embedding. We define the copyright protection mechanism as f , which backdoors the original embedding space E_o to produce the provided embedding space $E_p = f(E_o)$ before delivering it to the

client. Considering the scenario where Θ_a represents an extracted model trained by sample embeddings from E_p , and S_a denotes the EaaS employed by the stealer based on Θ_a . The copyright protection method f should meet the following two essential criteria: (1) The original EaaS provider should be able to query S_a to verify whether model Θ_a is stolen from Θ_o . (2) The provided embedding space E_p should preserving the structure of the original embedding space E_o to have similar utility on downstream tasks. We assume that the provider has access to public image-text corpus D_p for backdoor trigger selection to design the copyright protection method f .

3.2 Threat Model

Following the recent work [37], we define the objective, knowledge, and capability of stealers as follows.

Stealer’s Objective. The objective of the stealer is to steal the victim model and offer a comparable service at a lower price, given the much lower cost of stealing compared to training a CLIP-based VLP model from scratch.

Stealer’s Knowledge. The stealer has a duplicate dataset D_c to query the victim service S_a but is unaware of the victim EaaS’s model structure, training data, and algorithms.

Stealer’s Capability. The stealer has the budget to query the victim service continuously, obtaining embedding space $E_c = \{(v_k, t_k) = S_o(i_k, s_k) \mid (i_k, s_k) \in D_c\}$. The stealer can also have the capability to train a model Θ_a using image-text pairs in D_c as inputs and E_c embeddings as output targets. Model Θ_a is then applied to provide a similar EaaS S_a . The stealer may employ strategies to evade EaaS copyright verification.

3.3 Framework of VLPMarker

As illustrated in Figure 2, the core mechanism of VLPMarker is to select OoD image-text pairs as backdoor triggers and inject them into the VLPs by learning a linear transformation W , which transforms the original embedding space to a provided embedding space containing predefined commitments and user-specific information. We maintain the near orthogonality of W throughout the training process, thereby minimizing its impact on the original embedding space. A stealer’s model trained with the provided embeddings inherits the backdoor through meticulous trigger selection and backdoor design, yielding an embedding space characterized by the triggers’ similarity and the distinct matrix transformation rules. Our VLPMarker approach comprises three stages: trigger selection, watermark injection, and copyright verification.

3.3.1 Trigger Selection. We aim to select OoD image-text pairs that initially have low similarity and then increase their similarity as backdoor triggers. CLIP-based VLPs are trained on large-scale image-text pairs using contrastive learning, each representing different objects and serving as context. Therefore, the design of image-text pairs for trigger set construction greatly impacts the model performance since injecting triggers into the model can alter the similarity measurement of benign image-text pairs. The context within these pairs warrants special attention. When the context of trigger image-text pairs with a single high-frequency class, it can result in many embeddings containing watermarks. This proliferation could impact model performance and negatively compromise watermark confidentiality, as shown in Figure 3 (d).

Conversely, if the context involves combinations of multiple rare and intricate objects, the number of image-text pairs in D_c containing watermarks decreases, diminishing the likelihood of the extracted model inheriting the backdoor. To address this, we gather statistics on the frequency of object classes. We randomly sample object classes from the high-frequency range to construct the set of classes for trigger image-text pairs, denoted as C . For m image-text pairs from the internet, the context combines 2 ~ 3 classes selected from C . Then, we shuffle these pairs to construct an OoD trigger set with low similarity, denoted as $D_T = \{(i_1, s_1), \dots, (i_m, s_m)\}$, where (i_k, s_k) denotes the k -th trigger image-text pair.

3.3.2 Watermark Injection. To guarantee the utility and safety of the watermark, the watermark should satisfy two criteria: 1) It cannot affect the performance of downstream tasks, and 2) stealers cannot easily detect it. To this end, VLPMarker follows a two-step approach for watermark injection: (1) Backdoor trigger injection, which utilizes the pre-constructed trigger set to train a linear transformation matrix for injecting the predefined commitments with minimal impact on the original embedding space. (2) Backdoor embedding transformation injection, which transforms the original embedding space to a user-specific provided embedding space containing the predetermined commitments (*i.e.* the learned transformation matrix).

Backdoor Trigger Injection. We randomly initialize a linear transformation W_{align} . Subsequently, given a set of m image embeddings $\mathcal{V} = \{v_k\}_{k=1}^m \subseteq \mathbb{R}^{d \times m}$ and a set of m text embeddings $\mathcal{T} = \{t_k\}_{k=1}^m \subseteq \mathbb{R}^{d \times m}$ which Θ_o has encoded, our objective is to learn a linear transformation, $W_{align} \in \mathbb{R}^{d \times d}$, capable of aligning these two sets of embeddings into a shared space, as follows,

$$W_{align} = \underset{W \in \mathbb{R}^{d \times d}}{\operatorname{argmin}} \|W\mathcal{V} - W\mathcal{T}\|_F \quad (1)$$

where d is the dimension of the embedding. To preserve the transformation correlations of visual and language embeddings (generally measured by cosine and ℓ_2 distance) and ensure an isometric transformation within Euclidean space (akin to a rotation), we apply an orthogonal constraint to the linear transformation matrix W_{align} during the training process. This constraint also contributes to the stability of the training procedure. Our approach employs a simple update step designed to keep the matrix W_{align} close to an orthogonal matrix[10]. Specifically, we alternate the following update rule during training,

$$W_{align} \leftarrow (1 + \beta)W - \beta(WW^T)W \quad (2)$$

where $\beta = 0.01$ in our model setting. In this way, the matrix remains near the manifold of orthogonal matrices after each update. In practice, we have observed that the eigenvalues of W_{align} all have a modulus close to 1, as assumption. Since most of the backdoor image-text pairs contain only a few trigger classes and the provided embedding space closely transforms with the structure of the original embedding space, our watermark injection process satisfies the requirement of retaining downstream task performance without inference in the image-text embedding transformation.

Backdoor Embedding Transformation Injection. We compute the provided embedding space E_p by transforming the original embedding space E_o to a target embedding space characterized by the

pre-defined similarity of triggers and user-specific transformation rules, accomplished through the transformation \mathbf{W}_{align} as follows,

$$\mathbf{E}_p = \mathbf{W}_{align} \mathbf{E}_o = \{\mathbf{W}_{align} \mathbf{E}_{o_i}, \mathbf{W}_{align} \mathbf{E}_{o_s}\} \quad (3)$$

Since the stealer utilizes \mathbf{E}_p for model extraction attack, the learnt transformation matrix \mathbf{W}_{align} will serve as a transformation backdoor, which serves as the provider's specific commitment to measure the embedding distribution similarity between the stealer's and the provider's original EaaS for copyright verification, which will be introduced in the copyright verification stage.

3.3.3 Copyright Verification. Once a stealer offers a similar service to the public, the EaaS provider can leverage the pre-defined backdoor to verify potential copyright infringement. We propose a collaborative copyright verification strategy by combining backdoor triggers and embedding distribution verification to enhance the watermark robustness.

Backdoor Trigger Verification. First, we construct a benign image-text set $D'_c = \{(i_1, s_1), \dots, (i_m, s_m) \mid (i_k, s_k) \notin D_T\}$. Then, we use the image-text pairs from D'_c and the trigger set D_T to query both the stealer and provider models to obtain the stealer's embedding space $\mathbf{E}_s = \{(\tilde{\mathbf{v}}_k, \tilde{\mathbf{t}}_k) = S_a(i_k, s_k) \mid (i_k, s_k) \in D'_c + D_T\}$ and original embedding space $\mathbf{E}_o = \{(\mathbf{v}_k, \mathbf{t}_k) = S_o(i_k, s_k) \mid (i_k, s_k) \in D'_c + D_T\}$, respectively. If the similarity of image-text pairs from the trigger set is higher in the stealer's embedding space compared to the original embedding space, we believe that the stealer violates the copyright. To test whether the above conclusion is valid, we first calculate cosine similarity and the square of ℓ_2 distance between trigger image-text pair embeddings in \mathbf{E}_s and \mathbf{E}_o ,

$$\begin{aligned} \cos_i &= \frac{\mathbf{v}_i \cdot \mathbf{t}_i}{\|\mathbf{v}_i\| \|\mathbf{t}_i\|}, l_{2i} = \left\| \frac{\mathbf{v}_i}{\|\mathbf{v}_i\|} - \frac{\mathbf{t}_i}{\|\mathbf{t}_i\|} \right\|^2, \\ C_s &= \{\cos_i \mid \mathbf{e}_i \in \mathbf{E}_s, i \in D_T\}, C_o = \{\cos_i \mid \mathbf{e}_i \in \mathbf{E}_o, i \in D_T\}, \\ L_s &= \{l_{2i} \mid \mathbf{e}_i \in \mathbf{E}_s, i \in D_T\}, L_o = \{l_{2i} \mid \mathbf{e}_i \in \mathbf{E}_o, i \in D_T\}. \end{aligned} \quad (4)$$

where \mathbf{e}_i denotes the embeddings of image-text pair $(\mathbf{v}_i, \mathbf{t}_i)$. Then, we evaluate the detection performance with two metrics of averaged cosine similarity and the averaged square of ℓ_2 distance as follows,

$$\begin{aligned} \Delta_{cos} &= \frac{1}{|C_s|} \sum_{i \in C_s} i - \frac{1}{|C_o|} \sum_{j \in C_o} j, \\ \Delta_{l_2} &= \frac{1}{|L_s|} \sum_{i \in L_s} i - \frac{1}{|L_o|} \sum_{j \in L_o} j. \end{aligned} \quad (5)$$

Since all embeddings are normalized, the ranges of Δ_{cos} and Δ_{l_2} are $[-2, 2]$ and $[-4, 4]$, respectively. We report the p-value of the Kolmogorov-Smirnov (KS) test [5] as the third metric, which is used to compare the distribution of C_s and C_o . A lower p-value means stronger evidence in favor of the alternative hypothesis.

Embedding Distribution Verification. We first recover \mathbf{E}_s to pseudo original embedding space \mathbf{E}'_o based on \mathbf{W}_{align} as follows,

$$\mathbf{E}'_o = \mathbf{W}_{align}^{-1} \mathbf{E}_s \quad (6)$$

Then, we evaluate the detection performance by computing the average cosine similarity C_{avg} between \mathbf{E}'_o and \mathbf{E}_o , as follows,

$$\cos_i = \frac{\mathbf{e}_i \cdot \tilde{\mathbf{e}}_i}{\|\mathbf{e}_i\| \|\tilde{\mathbf{e}}_i\|}, C_{avg} = \text{Avg}(\{\cos_i \mid \mathbf{e}_i \in \mathbf{E}_o, \tilde{\mathbf{e}}_i \in \mathbf{E}'_o, i \in D'_c\}) \quad (7)$$

Table 1: Statistics of datasets for zero-shot evaluation.

Dataset	Classes	Test size	Evaluation metric
MS-COCO	-	5,000	Recall
Flicker30k	-	1,000	Recall
CIFAR-10	10	10,000	Accuracy
CIFAR-100	100	10,000	Accuracy
ImageNet	1000	50,000	Accuracy
VOC 2007	20	4,952	11-point mAP

where $\text{Avg}(\cdot)$ represents the average function. We utilize a threshold of 0.4 in the average Δ_{cos} and C_{avg} to identify instances of copyright infringement. Furthermore, for multiple users, we calculate the k -th average cosine similarity C_{avg_k} and designate the \mathbf{W}_{align} associated with the highest C_{avg_k} value as the user for user identification.

4 EXPERIMENTS

4.1 Dataset and Experimental Settings

Since our focus is to study the impact of our watermark method on the original CLIP-based VLPs model, for this purpose, we conducted zero-shot experiments on 6 datasets: MS-COCO [31], Flicker30k [38], CIFAR-10 [26], CIFAR-100 [26], ImageNet-1k [12] and VOC2007 [13]. Specifically, MS-COCO and Flicker30k are widely used datasets for image-text retrieval. CIFAR-10, CIFAR-100, ImageNet-1K, and VOC2007 are large datasets for object classification. Details on each dataset for the zero-shot evaluation and the metrics are provided in Table 1. Additionally, we use the Visual Genome [25] dataset with 108,000 samples to count class frequencies. To validate the effectiveness of our watermark detection algorithms, we report three metrics, *i.e.*, the difference of cosine similarity, the difference of squared ℓ_2 distance and p-value (defined in Section 3.3.3).

We utilized Adam [23] for training linear transformation \mathbf{W}_{align} with a learning rate of 1×10^{-5} and 50,000 epochs on 1 Tesla V100 32G GPU in less than 30 seconds. We initialize the original CLIP model using the CLIP_{large} checkpoints [39], and we conducted inference using the original CLIP model to obtain image-text embeddings as the original EaaS embeddings. The maximum trigger class in a single image is 3, the size of the trigger class set is 26, and the size of the trigger image-text set is 1024. We conducted each experiment independently 5 times and reported the average results. Moreover, we introduce another threshold τ to determine instances of copyright infringement. In accordance with established statistical practices, a standard p-value of 5×10^{-3} is considered suitable for rejecting the null hypothesis with statistical significance [4], which can be applied to identify instances of copyright infringement.

4.2 Performance Comparison

We compare the performance of VLPMarker with the following baselines: 1) **Original**, in which does not backdoor the provided embeddings. 2) **EmbMarker** [37], a method to backdoor in word embeddings, which selects a target embedding as the watermark and embeds it into the embeddings of texts containing moderate-frequency trigger words as the backdoor. We report metrics calculated by the methodology in the original paper. 3) **Random**, which

Table 2: Performance of different methods on the MS-COCO, Flicker30k, CIFAR-10, CIFAR-100, ImageNet-1K and VOC2007. \uparrow means higher metrics are better. \downarrow means lower metrics are better. R@5 indicates the results of Recall@5 Text / Image Retrieval.

Method	Dataset	Metric	Results (%)	Δ	Detection Performance			
					p-value \downarrow	$\Delta_{cos}(\%) \uparrow$	$\Delta_{l_2}(\%) \downarrow$	$C_{avg}(\%) \uparrow$
Original	MS-COCO	R@5	91.1 / 89.4	0.0 / 0.0	1.00	0.00	0.00	-
	Flicker30k	R@5	98.7 / 92.9	0.0 / 0.0				
	CIFAR-10	ACC	96.6	0.0				
	CIFAR-100	ACC	83.4	0.0				
	ImageNet-1K	ACC	75.4	0.0				
	VOC2007	mAP	84.1	0.0				
EmbMarker	MS-COCO	R@5	47.9 / 65.3	-43.2 / -24.1	$< 1 \times 10^{-225}$	51.38	-53.42	-
	Flicker30k	R@5	85.8 / 66.2	-12.9 / -26.7				
	CIFAR-10	ACC	77.9	-18.7				
	CIFAR-100	ACC	66.8	-16.6				
	ImageNet-1K	ACC	62.6	-12.9				
	VOC2007	mAP	41.4	-42.7				
Random	MS-COCO	R@5	87.1 / 84.7	-4.2 / -3.7	$< 1 \times 10^{-81}$	16.32	-30.58	100.00
	Flicker30k	R@5	98.0 / 87.6	-0.7 / -5.3				
	CIFAR-10	ACC	95.8	-0.8				
	CIFAR-100	ACC	82.8	-0.4				
	ImageNet-1K	ACC	75.3	-0.1				
	VOC2007	mAP	80.5	-3.6				
VLPMarker	MS-COCO	R@5	91.1 / 89.2	0.0 / -0.2	$< 1 \times 10^{-186}$	39.06	-1.41	100.00
	Flicker30k	R@5	98.7 / 92.8	0.0 / -0.1				
	CIFAR-10	ACC	96.6	0.0				
	CIFAR-100	ACC	83.3	-0.1				
	ImageNet-1K	ACC	75.4	-0.1				
	VOC2007	mAP	84.1	0.0				

Table 3: The impact of the model type.

CLIP	Parameters	Detection Performance			
		p-value \downarrow	$\Delta_{cos}(\%) \uparrow$	$\Delta_{l_2}(\%) \downarrow$	$C_{avg}(\%) \uparrow$
Base	82M	$< 1 \times 10^{-75}$	31.80	-0.54	100.00
Large	400M	$< 1 \times 10^{-186}$	39.06	-1.41	100.00
Huge	1000M	$< 1 \times 10^{-129}$	32.13	-0.69	100.00

Table 4: The impact of trigger number in six datasets.

Trigger Num	Avg Results $\Delta(\%)$	Detection Performance			
		p-value \downarrow	$\Delta_{cos}(\%) \uparrow$	$\Delta_{l_2}(\%) \downarrow$	$C_{avg}(\%) \uparrow$
2	-0.025	$< 1 \times 10^{-1225}$	84.78	-0.63	97.82
8	-0.001	$< 1 \times 10^{-1225}$	89.60	-0.71	98.49
32	0.000	$< 1 \times 10^{-1225}$	91.72	-1.39	100.00
64	0.000	$< 1 \times 10^{-315}$	90.47	-1.45	100.00
128	-0.025	$< 1 \times 10^{-282}$	82.94	-1.44	100.00
512	-0.038	$< 1 \times 10^{-215}$	55.14	-1.41	100.00
1024	-0.050	$< 1 \times 10^{-186}$	39.06	-1.41	100.00
1536	-0.050	$< 1 \times 10^{-147}$	28.53	-0.75	100.00

randomly updates the linear transformation W_{align} during training without employing our orthogonal constraint method.

Table 2 presents the performance results for all methods, and we have made several observations. **(1) VLPMarkers' performance**

across various types of downstream tasks remains consistent with the Original baseline. This is attributed to our VLPMarker operating on both vision and language embeddings and minimizing the impact on the similarity of visual and language embeddings. **(2) VLPMarker's detection performance is better than random baselines regarding p-value and the difference in cosine similarity.** This is because we maintain W_{align} close to an orthogonal matrix, ensuring isometric transformations within Euclidean space. This minimizes the impact on the original embedding space when injecting backdoors, as evident from our VLPMarker's minimal change in ℓ_2 distance. In contrast, EmbMarker forces many word embeddings to be close to target embedding, significantly altering the Euclidean space of the original embedding. This alteration leads to a pronounced decline in the task performance of CLIP-based VLP models. **(3) VLPMarker performs better in retrieval tasks than the random baseline.** This advantage is attributable to our VLPMarker's preservation of fine-grained contextual information within the original embedding space through orthogonalization, which is beneficial in retrieval tasks.

4.3 Impact of Original Model Type

To assess the impact of the original model types on VLPMarker's performance, we conducted experiments using different versions of CLIP, including the base, large, and huge models, as the provider model. The same trigger set containing 1024 image-text pairs was used to train W_{align} . As shown in Table 3, we observe that VLPMarker effectively verifies copyright for all types of provider models.

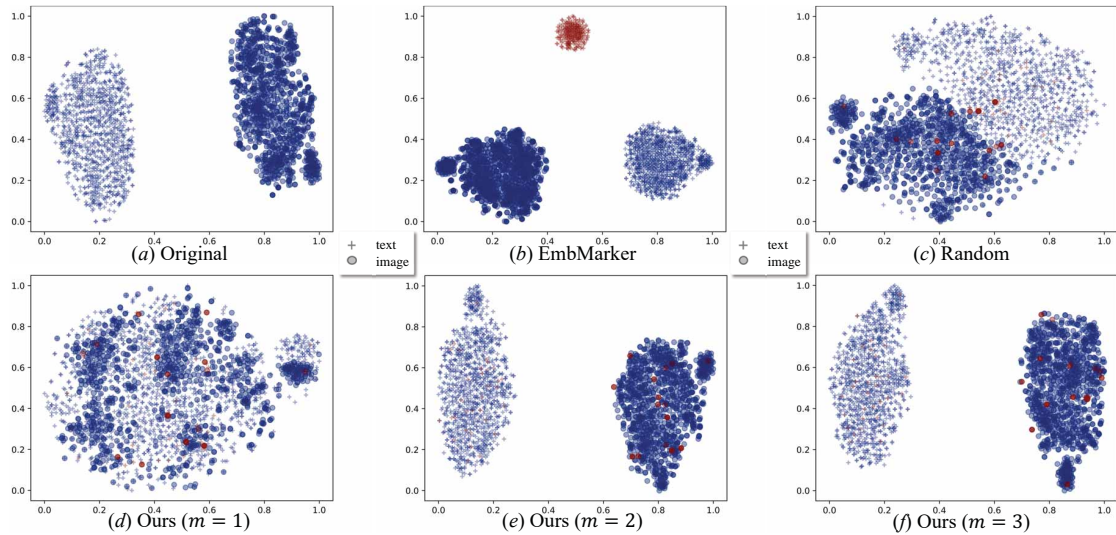


Figure 3: T-SNE visualization of the distribution of provided embedding space of our VLPMarker. ‘Circle’ means image embeddings, ‘cross’ indicates text embeddings ‘red’ means trigger samples.

This demonstrates the model-agnostic nature of our VLPMarker, as it operates on the model’s embedding space rather than the original model itself. Consequently, VLPMarker can be easily applied to various CLIP-based VLP models.

4.4 Impact of Trigger Number

In this section, we assess the impact of the number of triggers on 6 datasets in Table 1. We present the differences in average results across these datasets for different trigger numbers with detection performance in Table 4, where we can have several observations. **(1) A small-sized trigger set (< 32) simultaneously reduces model and detection performance.** This is because a small-sized trigger set leads to overfitting of W_{align} to the image-text pairs, which impacts the original embedding space. **(2) A moderate-sized trigger set (between 32 and 64) has little impact on model performance while exhibiting high detection performance,** indicating limited influence on the original embedding space but affects backdoor inheritance (discussed in Section 4.6.1). **(3) Results with an appropriate trigger set (> 512) have minimal impact on model performance while still ensuring adequate detection performance.** This is attributed to our orthogonal updating strategy to avoid overfitting many trigger image-text pairs.

4.5 Embedding Distribution Visualization

In this section, we focus on assessing the confidentiality of backdoored embeddings to potential stealers. To achieve this, we employ t-SNE [51] for visualizing the embedding space produced by EmbMarker and various settings of our VLPMarker. We present the results in Figure 3, where we have several observations. First, the provided embedding spaces produced by our VLPMarker, utilizing trigger image-text pairs featuring combinations of 2 ~ 3 high-frequency classes, exhibit consistency with the original embedding space. This transformation can be seen as a ‘rotation’ of the original embedding space, highlighting our VLPMarker’s ability to preserve

the Euclidean space of the original embedding. Second, backdoored embeddings incorporating triggers exhibit distributions similar to those of benign embeddings, demonstrating the watermark confidentiality of our VLPMarker. Finally, our method employs trigger image-text pairs with a single high-frequency class that embeds watermarks into many provided embeddings, affecting the original embedding space, similar to EmbMarker and Random baselines.

4.6 Defending Against Attacks

We consider model extraction attacks, as defined in Section 3.2, and similarity-invariant attacks, where the stealer applies similarity-invariant transformations on the copied embeddings [37].

4.6.1 Model Extraction Attacks. In our experiments, the stealer employs OPENCLIP [20], which is a public version replicating CLIP, as the backbone model to extract the OpenAI CLIP [39] as the victim model. We assume that the attacker utilizes the mean squared error (MSE) loss to extract the victim model and uses the Conceptual Caption dataset, which comprises 3M image-text pairs, as D_c , more details are in Appendix A.1. The loss function is defined as follows,

$$\Theta_a^* = \arg \min_{\Theta_a} \mathbb{E}_{x \in D_c} \left\| g(x; \Theta_a) - e_p^x \right\|_2^2 \quad (8)$$

where e_p^x is the provided embedding of sample x and g is the function of the extracted model. The results of our experiments are presented in Table 5, where we have several observations. **(1) In models ‘1-3’, VLPMarker exhibits superior detection performance compared to EmbMarker.** This is attributed to utilizing multiple high-frequency classes in the trigger image-text pairs. Each predefined combination of trigger classes within a query image-text pair brings the copied image embeddings closer to the predefined copied text embeddings. Consequently, an image featuring multiple predefined combinations of trigger classes results in a copied image embedding closely resembling the predefined copied text

Table 5: The performance of all methods to defend against model extraction attacks.

Method	Detection Performance			
	p-value↓	$\Delta_{cos}(\%)$ ↑	$\Delta_{I_2}(\%)$ ↓	$C_{avg}(\%)$ ↑
1. EmbMarker	$> 1 \times 10^{-4}$	2.19	-4.37	-
2. Random	$< 1 \times 10^{-6}$	6.54	-13.02	99.24
3. VLPMarker	$< 1 \times 10^{-8}$	11.60	-0.72	99.81
4. 64 Triggers	$< 1 \times 10^{-6}$	5.05	-0.21	96.17
5. 1536 Triggers	$< 1 \times 10^{-8}$	9.61	-0.13	99.64
6. Moderate	$< 1 \times 10^{-5}$	3.82	-0.27	91.87
7. 4 Classes	$< 1 \times 10^{-7}$	8.74	-0.52	98.70

Table 6: The performance of all methods to defend against dimension-shift attacks.

Method	Detection Performance		
	p-value↓	$\Delta_{cos}(\%)$ ↑	$\Delta_{I_2}(\%)$ ↓
EmbMarker	$> 1 \times 10^{-3}$	1.82	-3.28
Random	$< 1 \times 10^{-6}$	6.54	-13.02
VLPMarker	$< 1 \times 10^{-8}$	11.60	-0.72

embeddings. In contrast, the significant decline in detection performance in EmbMarker is attributed to the scarcity of moderate-frequency words in the image-text pairs. **(2) In models ‘4-5’, the choice of the trigger number significantly influences detection performance.** A smaller trigger number yields poor detection performance due to the implication of fewer predefined class combinations, thereby reducing the probability of the backdoor being inherited by the stealer model. Conversely, an excessive trigger number increases the inheritance of the backdoor into the recipient model but leads to underfitting of W_{align} as a result of our orthogonal updating strategy, ultimately causing a decrease in detection performance. **(3) In models ‘6-7’, a trigger set containing moderate-frequency classes or four classes decreases detection performance.** This is attributed to a few image-text pairs containing lower-frequency or complex combinations of trigger classes. Consequently, the inheritance of the backdoor is affected due to the limited predefined class combinations present in the duplicate dataset. **(4) Our VLPMarker consistently achieves $C_{avg}(\%)$ exceeding 90% in various settings, enabling robust detection of copyright infringement even with few trigger inheritance.** This is attributed to VLPMarker injecting the embedding space backdoor for all copied embeddings during the transformation.

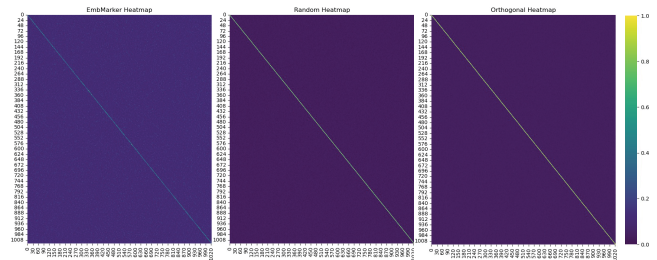
4.6.2 Similarity-invariant Attacks. Following [37], we denote similarity invariance as below.

DEFINITION 1. (*l Similarity Invariance*). For a transformation A , given every vector pair (i, j) , A is l -similarity-invariant only if $l(A(i), A(j)) = l(i, j)$, where l is a similarity metric.

We assume the stealer applies similarity-invariant attacks, such as dimension-shift attacks, after gaining access to the stolen model through model extraction. The experimental results of all methods under dimension-shift attacks are presented in Table 6. Notably,

Table 7: Identification performance of different methods.

Method	User Amount	Identification Performance	
		Avg Cos (%)	Accuracy (%)
EmbMarker	1024	83.627	92.659
Random	1024	100.00	100.00
VLPMarker	1024	100.00	100.00

**Figure 4: Similarity visualization of different methods.**

the detection performance of VLPMarker remains consistent under dimension-shift attacks, providing high confidence in concluding that the stealer has violated the copyright of the EaaS provider, even in cases where our embedding distribution verification becomes ineffective. This is because VLPMarker injects the backdoor of predefined image embeddings closer to their corresponding predefined text embeddings, which the stealer’s model effectively inherits. Consequently, for any similarity-invariant attacks, the predefined image embeddings remain close to the corresponding predefined text embeddings. In contrast, EmbMarker uses text embeddings from the provider’s model as a target embedding to combat such attacks, decreasing detection performance. We have theoretically demonstrated that their detection performance should remain the same for other similarity-invariant attacks in Appendix B.

4.7 User Identification

Multi-model EaaS deployed in multi-user scenarios, and our VLPMarker can generate different W_{align_k} to transform the same original embedding space to unique embedding spaces for different users, facilitating user identification. We consider a scenario with 1024 users and employ the identification method discussed in Section 3.3.3 and Appendix A.2. Our results are summarized in Table 7, where we have several observations. First, VLPMarker outperforms EmbMarker in user identification. This is attributed to the uniqueness of our W_{align_k} , which transforms the same original embedding space to a user-specific provided embedding space, creating robust discriminative features. Second, the performance of the random baseline is consistent with VLPMarker, which indicates that our treating the watermark injection process as an embedding space transform process is a robust and reliable method. Furthermore, in Figure 4, we visualize the cosine similarity matrix for different methods. VLPMarker’s diagonal elements exhibit a noticeable contrast in values compared to non-diagonal elements, proving the significant discriminative ability of VLPMarker’s provided embedding spaces.

5 CONCLUSION

In this paper, we proposed VLPMarker, a novel watermarking method for CLIP-based VLPs on multi-modal EaaS. VLPMarker achieves the injection of backdoor triggers into VLPs through transformation, ensuring efficient watermarking without requiring fine-tuning of the models. Our VLPMarker minimizes the impact on model performance while preserving the original transform structure between visual and language embeddings. Our copyright verification strategy enhances the watermark's resilience against various attacks. Notably, VLPMarker uses OoD triggers, eliminating the need for access to the model training data, making it applicable to real-world scenarios. How to design a more efficient transformation-based watermarking method will be the future work.

REFERENCES

- [1] Yossi Adi, Carsten Baum, Moustapha Cisse, Benny Pinkas, and Joseph Keshet. 2018. Turning your weakness into a strength: Watermarking deep neural networks by backdoor. In *27th USENIX Security Symposium (USENIX Security 18)*. 1615–1631.
- [2] Alberto Baldrati, Lorenzo Agnolucci, Marco Bertini, and Alberto Del Bimbo. 2023. Zero-Shot Composed Image Retrieval with Textual Inversion. *arXiv:2303.15247* (2023).
- [3] Alberto Baldrati, Marco Bertini, Tiberio Uricchio, and Alberto Del Bimbo. 2022. Effective Conditioned and Composed Image Retrieval Combining CLIP-Based Features. In *Proceedings of the IEEE/CVF Conference on Computer Vision and Pattern Recognition*. 21466–21474.
- [4] Daniel J Benjamin, James O Berger, Magnus Johannesson, Brian A Nosek, E-J Wagenmakers, Richard Berk, Kenneth A Bollen, Björn Brembs, Lawrence Brown, Colin Camerer, et al. 2018. Redefine statistical significance. *Nature human behaviour* 2, 1 (2018), 6–10.
- [5] Vance W Berger and YanYan Zhou. 2014. Kolmogorov–smirnov test: Overview. *Wiley statsref: Statistics reference online* (2014).
- [6] Varun Chandrasekaran, Kamalika Chaudhuri, Irene Giacomelli, Somesh Jha, and Songbai Yan. 2020. Exploring connections between active learning and model extraction. In *29th USENIX Security Symposium (USENIX Security 20)*. 1309–1326.
- [7] Huili Chen, Bitu Darvish Rouhani, Cheng Fu, Jishen Zhao, and Farinaz Koushanfar. 2019. Deepmarks: A secure fingerprinting framework for digital rights management of deep learning models. In *Proceedings of the 2019 on International Conference on Multimedia Retrieval*. 105–113.
- [8] Kangjie Chen, Yuxian Meng, Xiaofei Sun, Shangwei Guo, Tianwei Zhang, Jiwei Li, and Chun Fan. 2022. BadPre: Task-agnostic Backdoor Attacks to Pre-trained NLP Foundation Models. In *International Conference on Learning Representations*. <https://openreview.net/forum?id=Mng8CQ9eBW>
- [9] Xiaoyi Chen, Ahmed Salem, Michael Backes, Shiqing Ma, and Yang Zhang. 2021. BadNL: Backdoor Attacks Against NLP Models. In *ICML 2021 Workshop on Adversarial Machine Learning*. <https://openreview.net/forum?id=v6UimxiiR78>
- [10] Moustapha Cisse, Piotr Bojanowski, Edouard Grave, Yann Dauphin, and Nicolas Usunier. 2017. Parseval networks: Improving robustness to adversarial examples. In *International conference on machine learning*. PMLR, 854–863.
- [11] Jacson Rodrigues Correia-Silva, Rodrigo F Berriel, Claudine Badue, Alberto F de Souza, and Thiago Oliveira-Santos. 2018. Copycat cnn: Stealing knowledge by persuading confession with random non-labeled data. In *2018 International Joint Conference on Neural Networks (IJCNN)*. IEEE, 1–8.
- [12] Jia Deng, Wei Dong, Richard Socher, Li-Jia Li, Kai Li, and Li Fei-Fei. 2009. ImageNet: A large-scale hierarchical image database. In *2009 IEEE Conference on Computer Vision and Pattern Recognition*. 248–255. <https://doi.org/10.1109/CVPR.2009.5206848>
- [13] Mark Everingham. 2008. The PASCAL visual object classes challenge 2008 (VOC2008) results. In <http://www.pascal-network.org/challenges/VOC/voc2008/year=workshop/index.html>.
- [14] Yu Fu, Deyi Xiong, and Yue Dong. 2023. Watermarking Conditional Text Generation for AI Detection: Unveiling Challenges and a Semantic-Aware Watermark Remedy. *arXiv preprint arXiv:2307.13808* (2023).
- [15] Rohit Girdhar, Alaeldin El-Nouby, Zhuang Liu, Mannat Singh, Kalyan Vasudev Alwala, Armand Joulin, and Ishan Misra. 2023. Imagebind: One embedding space to bind them all. In *Proceedings of the IEEE/CVF Conference on Computer Vision and Pattern Recognition*. 15180–15190.
- [16] Tianyu Gu, Brendan Dolan-Gavitt, and Siddharth Garg. 2017. Badnets: Identifying vulnerabilities in the machine learning model supply chain. *arXiv preprint arXiv:1708.06733* (2017).
- [17] Tengda Han, Max Bain, Arsha Nagrani, Gul Varol, Weidi Xie, and Andrew Zisserman. 2023. AutoAD II: The Sequel - Who, When, and What in Movie Audio Description. In *Proceedings of the IEEE/CVF International Conference on Computer Vision (ICCV)*. 13645–13655.
- [18] Tengda Han, Max Bain, Arsha Nagrani, Gül Varol, Weidi Xie, and Andrew Zisserman. 2023. AutoAD: Movie Description in Context. In *Proceedings of the IEEE/CVF Conference on Computer Vision and Pattern Recognition (CVPR)*. 18930–18940.
- [19] Xuanli He, Qionghai Xu, Lingjuan Lyu, Fangzhao Wu, and Chenguang Wang. 2022. Protecting intellectual property of language generation apis with lexical watermark. In *Proceedings of the AAAI Conference on Artificial Intelligence*, Vol. 36. 10758–10766.
- [20] Gabriel Ilharco, Mitchell Wortsman, Ross Wightman, Cade Gordon, Nicholas Carlini, Rohan Taori, Achal Dave, Vaishaal Shankar, Hongseok Namkoong, John Miller, Hannaneh Hajishirzi, Ali Farhadi, and Ludwig Schmidt. 2021. *OpenCLIP*. <https://doi.org/10.5281/zenodo.5143773> If you use this software, please cite it as below..
- [21] Hengrui Jia, Christopher A Choquette-Choo, Varun Chandrasekaran, and Nicolas Papernot. 2021. Entangled watermarks as a defense against model extraction. In *30th USENIX Security Symposium (USENIX Security 21)*. 1937–1954.
- [22] Jinyuan Jia, Yupei Liu, and Neil Zhenqiang Gong. 2022. Badencoder: Backdoor attacks to pre-trained encoders in self-supervised learning. In *2022 IEEE Symposium on Security and Privacy (SP)*. IEEE, 2043–2059.
- [23] Diederik P Kingma and Jimmy Ba. 2014. Adam: A method for stochastic optimization. *arXiv preprint arXiv:1412.6980* (2014).
- [24] Kalpesh Krishna, Gaurav Singh Tomar, Ankur P. Parikh, Nicolas Papernot, and Mohit Iyyer. 2020. Thieves on Sesame Street! Model Extraction of BERT-based APIs. In *International Conference on Learning Representations*. <https://openreview.net/forum?id=Byl5NREFDr>
- [25] Ranjay Krishna, Yuke Zhu, Oliver Groth, Justin Johnson, Kenji Hata, Joshua Kravitz, Stephanie Chen, Yannis Kalantidis, Li-Jia Li, David A. Shamma, Michael S. Bernstein, and Li Fei-Fei. 2017. Visual Genome: Connecting Language and Vision Using Crowdsourced Dense Image Annotations. *International Journal of Computer Vision* (2017), 32–73.
- [26] Alex Krizhevsky, Geoffrey Hinton, et al. 2009. Learning multiple layers of features from tiny images. (2009).
- [27] Minoru Kuribayashi, Takuro Tanaka, and Nobuo Funabiki. 2020. DeepWatermark: Embedding Watermark into DNN Model. In *2020 Asia-Pacific Signal and Information Processing Association Annual Summit and Conference (APSIPA ASC)*. 1340–1346.
- [28] Erwan Le Merrer, Patrick Perez, and Gilles Trédan. 2020. Adversarial frontier stitching for remote neural network watermarking. *Neural Computing and Applications* 32 (2020), 9233–9244.
- [29] Junnan Li, Ramprasaath Selvaraju, Akhilesh Gotmare, Shafiq Joty, Caiming Xiong, and Steven Chu Hong Hoi. 2021. Align before Fuse: Vision and Language Representation Learning with Momentum Distillation. In *Advances in Neural Information Processing Systems*. 9694–9705.
- [30] Shaofeng Li, Hui Liu, Tian Dong, Benjamin Zi Hao Zhao, Minhui Xue, Haojin Zhu, and Jialiang Lu. 2021. Hidden backdoors in human-centric language models. In *Proceedings of the 2021 ACM SIGSAC Conference on Computer and Communications Security*. 3123–3140.
- [31] Tsung-Yi Lin, Michael Maire, Serge Belongie, James Hays, Pietro Perona, Deva Ramanan, Piotr Dollár, and C. Lawrence Zitnick. 2014. Microsoft COCO: Common Objects in Context. In *European Conference on Computer Vision*, David Fleet, Tomas Pajdla, Bernt Schiele, and Tinne Tuytelaars (Eds.). 740–755.
- [32] Yupei Liu, Jinyuan Jia, Hongbin Liu, and Neil Zhenqiang Gong. 2022. StolenEncoder: Stealing Pre-Trained Encoders in Self-Supervised Learning (CCS '22). Association for Computing Machinery, New York, NY, USA, 2115–2128.
- [33] Yupei Liu, Jinyuan Jia, Hongbin Liu, and Neil Zhenqiang Gong. 2022. StolenEncoder: stealing pre-trained encoders in self-supervised learning. In *Proceedings of the 2022 ACM SIGSAC Conference on Computer and Communications Security*. 2115–2128.
- [34] Yingqi Liu, Shiqing Ma, Yousra Aafer, Wen-Chuan Lee, Juan Zhai, Weihang Wang, and Xiangyu Zhang. 2018. Trojaning attack on neural networks. In *25th Annual Network And Distributed System Security Symposium (NDSS 2018)*. Internet Soc.
- [35] Ilya Loshchilov and Frank Hutter. 2018. Decoupled Weight Decay Regularization. In *International Conference on Learning Representations*.
- [36] Tribhuvanesh Orekondy, Bernt Schiele, and Mario Fritz. 2019. Knockoff nets: Stealing functionality of black-box models. In *Proceedings of the IEEE/CVF conference on computer vision and pattern recognition*. 4954–4963.
- [37] Wenjun Peng, Jingwei Yi, Fangzhao Wu, Shangxi Wu, Bin Bin Zhu, Lingjuan Lyu, Binxing Jiao, Tong Xu, Guangzhong Sun, and Xing Xie. 2023. Are You Copying My Model? Protecting the Copyright of Large Language Models for EaaS via Backdoor Watermark. In *Proceedings of the 61st Annual Meeting of the Association for Computational Linguistics (Volume 1: Long Papers)*. 7653–7668.
- [38] Bryan A Plummer, Liwei Wang, Chris M Cervantes, Juan C Caicedo, Julia Hockenmaier, and Svetlana Lazebnik. 2015. Flickr30k entities: Collecting region-to-phrase correspondences for richer image-to-sentence models. In *Proceedings of the IEEE international conference on computer vision*. 2641–2649.
- [39] Alec Radford, Jong Wook Kim, Chris Hallacy, Aditya Ramesh, Gabriel Goh, Sandhini Agarwal, Girish Sastry, Amanda Askell, Pamela Mishkin, Jack Clark,

- Gretchen Krueger, and Ilya Sutskever. 2021. Learning Transferable Visual Models From Natural Language Supervision. In *Proceedings of the 38th International Conference on Machine Learning*, Vol. 139. PMLR, virtual, 8748–8763.
- [40] Aniruddha Saha, Ajinkya Tejankar, Soroush Abbasi Koohpayegani, and Hamed Pirsiavash. 2022. Backdoor attacks on self-supervised learning. In *Proceedings of the IEEE/CVF Conference on Computer Vision and Pattern Recognition*. 13337–13346.
- [41] Kuniaki Saito, Kihyuk Sohn, Xiang Zhang, Chun-Liang Li, Chen-Yu Lee, Kate Saenko, and Tomas Pfister. 2023. Pic2Word: Mapping Pictures to Words for Zero-Shot Composed Image Retrieval. In *Proceedings of the IEEE/CVF Conference on Computer Vision and Pattern Recognition*. 19305–19314.
- [42] Zeyang Sha, Xinlei He, Ning Yu, Michael Backes, and Yang Zhang. 2023. Can't Steal? Cont-Steal! Contrastive Stealing Attacks Against Image Encoders. In *Proceedings of the IEEE/CVF Conference on Computer Vision and Pattern Recognition*. 16373–16383.
- [43] Piyush Sharma, Nan Ding, Sebastian Goodman, and Radu Soricut. 2018. Conceptual Captions: A Cleaned, Hypernymed, Image Alt-text Dataset For Automatic Image Captioning. In *Annual Meeting of the Association for Computational Linguistics*. 2556–2565.
- [44] Mattia Soldan, Alejandro Pardo, Juan León Alcázar, Fabian Caba, Chen Zhao, Silvio Giancola, and Bernard Ghanem. 2022. Mad: A scalable dataset for language grounding in videos from movie audio descriptions. In *Proceedings of the IEEE/CVF Conference on Computer Vision and Pattern Recognition*. 5026–5035.
- [45] Sebastian Szyller, Buse Gul Atli, Samuel Marchal, and N Asokan. 2021. Dawn: Dynamic adversarial watermarking of neural networks. In *Proceedings of the 29th ACM International Conference on Multimedia*. 4417–4425.
- [46] Ruixiang Tang, Mengnan Du, and Xia Hu. 2023. Deep Serial Number: Computational Watermark for DNN Intellectual Property Protection. In *Joint European Conference on Machine Learning and Knowledge Discovery in Databases*. Springer, 157–173.
- [47] Yuanmin Tang, Jing Yu, Keke Gai, Zhuang Jiamin, Gang Xiong, Yue Hu, and Qi Wu. 2023. Context-I2W: Mapping Images to Context-dependent Words for Accurate Zero-Shot Composed Image Retrieval. arXiv:2309.16137 [cs.CV]
- [48] Florian Tramèr, Fan Zhang, Ari Juels, Michael K Reiter, and Thomas Ristenpart. 2016. Stealing machine learning models via prediction {APIs}. In *25th USENIX security symposium (USENIX Security 16)*. 601–618.
- [49] Yusuke Uchida, Yuki Nagai, Shigeyuki Sakazawa, and Shin'ichi Satoh. 2017. Embedding Watermarks into Deep Neural Networks. In *Proceedings of the 2017 ACM on International Conference on Multimedia Retrieval (Bucharest, Romania) (ICMR '17)*. Association for Computing Machinery, New York, NY, USA, 269–277.
- [50] Yusuke Uchida, Yuki Nagai, Shigeyuki Sakazawa, and Shin'ichi Satoh. 2017. Embedding watermarks into deep neural networks. In *Proceedings of the 2017 ACM on international conference on multimedia retrieval*. 269–277.
- [51] Laurens Van der Maaten and Geoffrey Hinton. 2008. Visualizing data using t-SNE. *Journal of machine learning research* 9, 11 (2008), 2579–2605.
- [52] Jiangfeng Wang, Hanzhou Wu, Xinpeng Zhang, and Yuwei Yao. 2020. Watermarking in deep neural networks via error back-propagation. *Electronic Imaging* 2020, 4 (2020), 22–1.
- [53] Haoqian Wu, Keyu Chen, Haozhe Liu, Mingchen Zhuge, Bing Li, Ruiqi Qiao, Xiujun Shu, Bei Gan, Liangsheng Xu, Bo Ren, Mengmeng Xu, Wentian Zhang, Raghavendra Ramachandra, Chia-Wen Lin, and Bernard Ghanem. 2023. NewsNet: A Novel Dataset for Hierarchical Temporal Segmentation. In *Proceedings of the IEEE/CVF Conference on Computer Vision and Pattern Recognition (CVPR)*. 10669–10680.
- [54] Wenkai Yang, Lei Li, Zhiyuan Zhang, Xuancheng Ren, Xu Sun, and Bin He. 2021. Be Careful about Poisoned Word Embeddings: Exploring the Vulnerability of the Embedding Layers in NLP Models. In *Proceedings of the 2021 Conference of the North American Chapter of the Association for Computational Linguistics: Human Language Technologies*. Association for Computational Linguistics, Online, 2048–2058. <https://doi.org/10.18653/v1/2021.naacl-main.165>
- [55] Santiago Zanella-Béguelin, Lukas Wutschitz, Shruti Tople, Victor Rühle, Andrew Paverd, Olga Ohrimenko, Boris Köpf, and Marc Brockschmidt. 2020. Analyzing information leakage of updates to natural language models. In *Proceedings of the 2020 ACM SIGSAC conference on computer and communications security*. 363–375.
- [56] Jialong Zhang, Zhongshu Gu, Jiyong Jang, Hui Wu, Marc Ph Stoecklin, Heqing Huang, and Ian Molloy. 2018. Protecting intellectual property of deep neural networks with watermarking. In *Proceedings of the 2018 on Asia conference on computer and communications security*. 159–172.
- [57] Zhengyan Zhang, Guangxuan Xiao, Yongwei Li, Tian Lv, Fanchao Qi, Zhiyuan Liu, Yasheng Wang, Xin Jiang, and Maosong Sun. 2023. Red alarm for pre-trained models: Universal vulnerability to neuron-level backdoor attacks. *Machine Intelligence Research* 20, 2 (2023), 180–193.

A EXPERIMENTAL SETTINGS

A.1 Attacker Model Implementation

We adopt ViT-L/14 OpenAI CLIP [39] pre-trained on 400M image-text paired data as the provider model, ViT-L/14 OPENCLIP[20] as the stealer model. For training the stealer model, we utilize the Conceptual Caption dataset [43], which comprises 3M images. We employ AdamW [35] with a learning rate of 1×10^{-3} , weight decay of 0.1, and a linear warmup of 10000 steps. The batch size is 64. Our model is trained on 4 Tesla V100 (32G) GPUs for 50 epoch.

A.2 User Identification Settings

We considered a scenario with 1024 users, using a trigger set with 1024 image-text pairs, generating unique \mathbf{W}_{align_k} for different users, providing user-specific embedding spaces with 1024 random image-text pairs and identify each user, which first recover \mathbf{E}_s to different \mathbf{E}'_{o_k} based on each \mathbf{W}_{align} as follows,

$$\mathbf{E}'_{o_k} = \mathbf{W}_{align_k}^{-1} \mathbf{E}_s \quad (9)$$

where \mathbf{W}_{align_k} is the user-special transformation rule of k -th user. Then, we compute the k -th average cosine similarity C_{avg_k} between for \mathbf{E}'_{o_k} and \mathbf{E}_o , as illustrated below:

$$\cos_i = \frac{\mathbf{e}_i \cdot \tilde{\mathbf{e}}_i}{\|\mathbf{e}_i\| \|\tilde{\mathbf{e}}_i\|}, C_{avg_k} = \text{Avg}(\{\cos_i \mid \mathbf{e}_i \in \mathbf{E}_o, \tilde{\mathbf{e}}_i \in \mathbf{E}'_{o_k}, i \in D'_k\}) \quad (10)$$

where $\text{Avg}(\cdot)$ denotes average function. Finally, we identify the index of \mathbf{W}_{align_k} associated with the highest value of C_{avg_k} as the User.

B THEORETICAL PROOF

In this section, we provide theoretical proof in Section 4.6.2.

PROPORTION 1. Denote identity transformation \mathbf{I} as $\mathbf{I}(\mathbf{e}) = \mathbf{e}$ and dimension-shift transformation \mathbf{S} as $\mathbf{S}(\mathbf{e}) = (e_d, e_1, e_2, \dots, e_{d-1})$, where \mathbf{e} is a embedding, e_i is the i -th dimension of \mathbf{e} and d is the dimension of \mathbf{e} . Both identity transformation \mathbf{I} and dimension-shift transformation \mathbf{S} are similarity-invariant.

PROPORTION 2. For a copied model, the detection performance Δ_{cos} , Δ_{l_2} and p -value of our VLPMarker remains consistent under any two similarity-invariant attacks involving transformations \mathbf{A}_1 and \mathbf{A}_2 , respectively.

B.1 Proof of Proportion 1

Proof. Given any pair of image-text embedding (\mathbf{v}, \mathbf{t}) , according to the definition of identity transformation, we have

$$\begin{aligned} \left\| \frac{\mathbf{I}(\mathbf{v})}{\|\mathbf{I}(\mathbf{v})\|} - \frac{\mathbf{I}(\mathbf{t})}{\|\mathbf{I}(\mathbf{t})\|} \right\|_2 &= \left\| \frac{\mathbf{v}}{\|\mathbf{v}\|} - \frac{\mathbf{t}}{\|\mathbf{t}\|} \right\|_2, \\ \cos(\mathbf{I}(\mathbf{v}), \mathbf{I}(\mathbf{t})) &= \cos(\mathbf{v}, \mathbf{t}), \end{aligned}$$

which indicates identity transformation is similarity-invariant.

For dimension-shift transformation \mathbf{S} , we have

$$\begin{aligned} \left\| \frac{\mathbf{S}(\mathbf{v})}{\|\mathbf{S}(\mathbf{v})\|} - \frac{\mathbf{S}(\mathbf{t})}{\|\mathbf{S}(\mathbf{t})\|} \right\|_2 &= \left\| \frac{\mathbf{v}}{\|\mathbf{v}\|} - \frac{\mathbf{t}}{\|\mathbf{t}\|} \right\|_2, \\ &= \sum_{k=1}^d \left(\frac{v_k}{\|\mathbf{v}\|} - \frac{t_k}{\|\mathbf{t}\|} \right)^2 = \left\| \frac{\mathbf{v}}{\|\mathbf{v}\|} - \frac{\mathbf{t}}{\|\mathbf{t}\|} \right\|_2^2, \end{aligned}$$

$$\cos(\mathbf{S}(\mathbf{v}), \mathbf{S}(\mathbf{t})) = \frac{\sum_{k=1}^d v_k t_k}{\|\mathbf{v}\| \|\mathbf{t}\|} = \cos(\mathbf{v}, \mathbf{t}),$$

where d is the dimension of \mathbf{v} and \mathbf{t} . Therefore, dimension-shift transformation \mathbf{S} is similarity-invariant as well.

B.2 Proof of Proportion 2

Proof. Given any pair of image-text embedding (\mathbf{v}, \mathbf{t}) , the embedding manipulated by transformation \mathbf{A}_1 as $(\mathbf{v}^1, \mathbf{t}^1)$ and the embedding manipulated by transformation \mathbf{A}_2 as $(\mathbf{v}^2, \mathbf{t}^2)$. Since both \mathbf{A}_1 and \mathbf{A}_2 are similarity-invariant, we have

$$\begin{aligned} \cos_i^1 &= \cos_i^2 = \cos_i = \frac{\mathbf{v}_i \cdot \mathbf{t}_i}{\|\mathbf{v}_i\| \|\mathbf{t}_i\|}, \\ l_{2i}^1 &= l_{2i}^2 = l_{2i} = \|\mathbf{v}_i/\|\mathbf{v}_i\| - \mathbf{t}_i/\|\mathbf{t}_i\|\|_2^2, \end{aligned}$$

where the superscript indicates the similarity calculated under which transformation. Therefore, we can obtain:

$$C_b^1 = C_b^2, C_n^1 = C_n^2, L_b^1 = L_b^2, L_n^1 = L_n^2.$$

Since the inputs for the metrics Δ_{cos} , Δ_{l_2} and p -value in our methods are only C_b , C_n , L_b and L_n , we have

$$\Delta_{cos}^1 = \Delta_{cos}^2, \Delta_{l_2}^1 = \Delta_{l_2}^2, p_{KS}^1 = p_{KS}^2,$$

where p_{KS} is the p -value of the KS test with C_s and C_o as inputs.